2018 IEEE Intelligent Vehicles Symposium (IV)
Changshu, Suzhou, China, June 26-30, 2018

A Cooperative Vehicle Ego-localization Application Using V2V Communications with CBL Clustering

Lucas Rivoirard[1], Martine Wahl[1], Patrick Sondi[2], Dominique Gruyer[3] and Marion Berbineau[1]

***Abstract*— The cooperative vehicle paradigm offers new opportunities for enhancing various vehicle functions through distributed applications. The localization function is one of the most important since its services are needed by numerous applications ranging from driver navigation to autonomous vehicle guiding. Though the GPS (Global Positioning System) provides honorable service for driver navigation, its precision is not accurate for allowing an autonomous vehicle to localize itself correctly on the road lanes. Recently an ego-localization technique where a group of vehicles exchange their position and the related correction through V2V communications has been proposed in order to enhance the precision of the location of each node in the group. In this paper, we evaluate the performance that this application can expect from V2V communication services supplied by the CBL (Chain-Branch-Leaf) clustering scheme. The simulation results show that CBL achieves delays and packet delivery ratio adapted to various rates of the ego-localization application traffic.**

I. Introduction

Safety ITS (Intelligent Transportation System) applications, such as autonomous vehicle applications, will need accurate locations of vehicles. Global Positioning System (GPS) that currently provides the location information to each vehicle suffers from poor accuracy. Its typical errors are around 10 meters [1]. Although such performance is adequate for navigation, it is not sufficiently accurate for ITS safety application. For instance, it does not allow an on-board system to determine on which lane its vehicle is. Using further equipments information such as sensors (odometer, gyroscope, video, or image), base stations, or road maps, many techniques, reviewed in [2], provide positioning improvements to the GPS. One of theses techniques uses VANET links to exchange the position information from neighboring vehicles. This technique improves vehicle location by using cooperative map matching [3].

Among the literature proposals, [4] developed "a novel approach for improved vehicular positioning using Cooperative Map Matching" (CMM) and "Dynamic base station Differential GPS" (DDGPS) concept. But, this 2-step approach supposes that a VANET allows the vehicles to exchange data on their location and on the related error correction. This paper describes how the Chain-Branch-Leaf (CBL) clustering scheme developed for ad hoc communications in VANETs [5] offers the V2V communication services needed to the distributed cooperative location application described in [4].

The paper is organized as follows. Section II summarizes the two steps of the cooperative location algorithm, CMM and DDGPS, highlighting the variables to be shared within each vehicle neighborhood. Section III briefly presents the CBL clustering scheme, then section IV specifies the CMM and DDGPS messages exchanged by the vehicles to implement the distributed location application using CBL services. Section V shows the evaluations on the performance provided by CBL to the distributed location application in various road network traffic scenarios. We finally conclude the paper.

II. The CMM-DDGPS distributed location application

A GPS receiver is not sufficient to process vehicle ego-localization with the accuracy required by future automated vehicles. Differential GPS enhances the GPS positioning accuracy in using differential method exploiting fixed known position as a ground based reference, but it needs an expensive infrastructure deployment [4]. Therefore, [4] proposed "to extend the DGPS method by using mobile reference stations instead of a fixed one, thus generating pseudo-range corrections by nearby vehicles and broadcasting them to be used by nearby vehicles." Furthermore, before processing the Dynamic base station DGPS function, vehicles running the vehicular Cooperative Map Matching function have already given their GPS position by receiving position estimations from other vehicles and using them to better match their position to a precise lane level road map. We briefly present in the two following subsections the CMM and DDGPS functions and their requirements in terms of data transmission.

A. Communication requirements of the CMM function

The CMM function exploits the following property of the pseudorange noise: "the similarity of the common error components $\varsigma_j^{(i)}$ in pseudorange measurements $\rho_j^{(i)}$ from each satellite j to vehicles leads to the same bias in GPS position computed by each vehicle (i) in a vicinity" [4]. These pseudorange measurements are expressed as follows (equation 1):

$$\rho_j^{(i)} = D_j^{(i)} - c\delta t^{(i)} + \varsigma_j^{(i)} + \eta^{(i)} \quad (1)$$

where $D_j^{(i)}$ is the distance between the satellite j and the vehicle (i); c, the speed of the electromagnetic wave; $\delta t^{(i)}$, the clock synchronization error; and $\eta^{(i)}$, the no-common errors.

[1]Univ Lille Nord de France, IFSTTAR, COSYS, LEOST, F-59650 Villeneuve d'Ascq first-name.name@ifsttar.fr
[2]Univ. Littoral Côte d'Opale, LISIC - EA 4491, F-62228 Calais, France
[3]IFSTTAR, COSYS, LIVIC, F-78000 Versailles, France

The authors acknowledge the support of the CPER ELSAT2020 project which is co-financed by the European Union with the European Regional Development Fund, the French state and the Hauts de France Region Council.

To process the improvements by "vehicular cooperative map matching", [4] worked on the assumption that every vehicle on the road transmits its pseudorange values in a vicinity. Once the vehicle (i) measured the pseudorange $\rho_j^{(i)}$ from each received signal of a satellite j, the CMM algorithm computes its GPS position ($\tilde{X}^{(i)} = [\tilde{x}^{(i)}, \tilde{y}^{(i)}, \tilde{z}^{(i)}]$) and its position covariance, then it firstly restraints the uncertainty of its GPS position by applying its road constraints to that position. Next, receiving via a V2V link the pseudorange measures from a vehicle (v) in its neighborhood, computing both that vehicle GPS position $\tilde{X}^{(v)}$ and its position covariance, the vehicle (i) restraints again the uncertainty of its GPS position by applying the road map constraints of that vehicle to its own location. The author outlines that the map constraints of other vehicles are applicable to the vehicle (i) "only if the position of all vehicles are resolved using the same set of satellites". That way, the vehicle (i) successively improves its estimated position $\hat{X}^{(i)}$ from the knowledge of vehicle position in its vicinity.

Therefore, in terms of communication needs, the CMM function requires that each vehicle (i) broadcasts its pseudorange measurements $\rho_j^{(i)}$ for each visible satellite j in a vicinity.

B. Communication requirements of the DDGPS function

According to [4], the DDGPS function aims to enable each vehicle to correct its position estimation based on the shared knowledge of the error bias correction information for each visible satellite. To that purpose, each vehicle calculates a pseudorange correction $\Delta\rho_j^{(i)}$ for each visible satellite j and forwards it to its neighborhood (equation 2).

$$\Delta\rho_j^{(i)} = \hat{D}_j^{(i)} - \rho_j^{(i)} \tag{2}$$

where $\hat{D}^{(i)}$ is the geometric distance between the position of the satellite j and the position estimation $\hat{X}^{(i)}$ by (i); $\hat{X}^{(i)}$ can have previously been obtained with CMM or any positioning system. As a result, each receiver vehicle (r) can generate a set of differential pseudorange corrections $\rho_{j,corr}^{(i)}$ for every visible satellite j ($\rho_{j,corr}^{(i)} = \rho_j^{(r)} + \Delta\rho_j^{(i)}$).

However, it can happen that a vehicle (r) receives several pseudorange corrections from different vehicles for a same satellite j. In such a case, it has to merge them according to whether these data are independent or not in order to not lead to over-convergence. Therefore, DDGPS provides and transmits with each $\Delta\rho_j^{(i)}$ forwarded two more pieces of information: it computes the variance of the GPS pseudorange corrections $\sigma_j^{(i)}$ which describes the confident level parameter of the $\Delta\rho_j^{(i)}$ value; and it maintains for each computed $\Delta\rho_j^{(i)}$ a list of the vehicle identifier, including its own identifier, that have been involved in its calculation.

Thus, when a vehicle receives several set of pseudorange corrections, it can merge them after having checked that these data are independent: when the lists are not disjoint, the receiver vehicle (r) uses a weighted mean to merge the received corrections, it computes the new variance (see [4]), and it merges the identifier lists; but, when $\Delta\rho_j^{(i)}$ are dependent, DDGPS selects then the pseudorange correction that has the smallest $\sigma_j^{(i)}$, and next computes the weighted mean and the variance for the independent pseudorange corrections as previously.

Therefore, in terms of communication needs, the DDGPS function requires that for each vehicle (i) a message is forwarded containing for each correction information: the satellite identifiers j; the $\Delta\rho_j^{(i)}$ value; the $\sigma_j^{(i)}$ value; and the list of the vehicle identifiers that are involved in the $\Delta\rho_j^{(i)}$ correction.

III. The CBL clustering scheme

Previously, we presented in [5] the CBL cooperative clustering algorithm. CBL is a completely distributed algorithm where each communication node initiates its own process. It creates a hierarchy between the nodes in order to build 1-hop clusters. Each node of a cluster can directly communicate to the cluster-head without going through another intermediary node.

CBL defines two kinds of nodes (Fig. 1): branch nodes and leaf nodes. Both kinds of nodes emit periodic HELLO messages to build the CBL hierarchical structure. In that structure, connected branch nodes are links of a chain used to relay messages from branch to branch over long distance, up to their destination(s), upstream or downstream of the traffic flow. Typically, they are used to remote communication. Each branch node has its set of leaf nodes attached to it where close communication occurs. A set of leaf nodes and its attached branch node defines a 1-hop cluster. Two branch nodes linked are 1-hop neighbors.

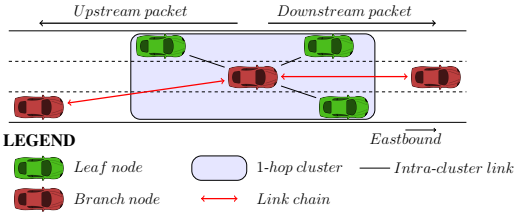

Fig. 1. Example of a node topology on a three-lane one-way highway

Each branch node is elected by other nodes (branch or leaf) in its 1-hop neighborhood. To build stable chains, CBL uses a metric called connection time (CT) or contact time. This metric which evaluates the duration of the connection between the network nodes is used by nodes to manage the election of their branch node.

IV. The adaptation of CMM and DDGPS to the CBL scheme

It is important to notice that the definition of branch and leaf nodes in the CBL scheme generates, at a given time, disjointed groups of nodes [5]. Each group is identifiable by its branch node. We propose to take advantage of that independence of groups of leaves, formed around the branch nodes, for DDGPS application. Therefore, we impose that:

- only leaf nodes (i) broadcast their pseudorange measurements $\rho_j^{(i)}$ in CMM message for each visible satellite j;
- branch nodes (i) are able to run both the CMM and DDGPS applications to compute the correction data for each satellite identifier j;
- branch nodes (i) are the only one allowed forwarding DDGPS messages, containing a set of pseudorange corrections $\Delta\rho_j^{(i)}$, to the upstream branch nodes and their leaf nodes.

In our implementation of the CMM-DDGPS applications, branch nodes play the role of the Dynamic base station Differential GPS. Restraining within each cluster the processing of the broadcasted $\rho_j^{(i)}$ to its branch node, then constraining each branch node to forward the correction messages to their cluster leaf nodes and only towards their upstream branch nodes, the chain structure of CBL helps to guarantee the independence of the correction data without needing to transfer for each set of pseudorange corrections the lists of the vehicle identifiers involved in the correction process. Therefore, DDGPS messages will contain only the following information for each correction: the satellite identifier j, $\sigma_j^{(i)}$, $\Delta\rho_j^{(i)}$ (IV-B).

A. Format of the CMM application message

The CMM application message is defined Fig. 2. It consists of several couples of 32-bit fields containing each one an identifier of a satellite (j) and the pseudorange value received by the (i) vehicle from that satellite $(\rho_j^{(i)})$. Thus, 64 bits code each satellite.

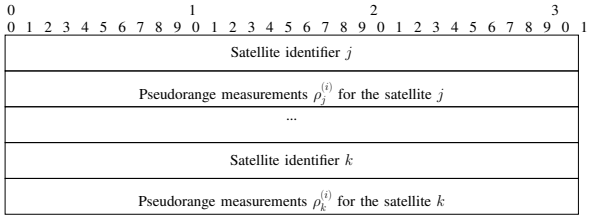

Fig. 2. Format of CMM application messages transmitted by leaf nodes

To realize the performance analysis of the CMM-DDGPS implementation on CBL scheme, CMM messages will be sent by unicast by the leaf nodes to their branch node in simulations (see IV-C).

B. Format of the DDGPS application message

The DDGPS application message is defined Fig. 3. It consists of several sets of three 32-bit fields containing each one an identifier of a visible satellite (j), the correction variance $(\sigma_j^{(i)})$ and the pseudorange correction $\Delta\rho_j^{(i)}$. Thus, 96 bits code each visible satellite.

C. CMM and DDGPS temporal interaction diagram

Fig. 4 illustrates a sequence of DDGPS and CMM application messages within a six-node VANET. Nodes 3, 5, and 6 are three successive branch nodes of a same chain; Node 3 is

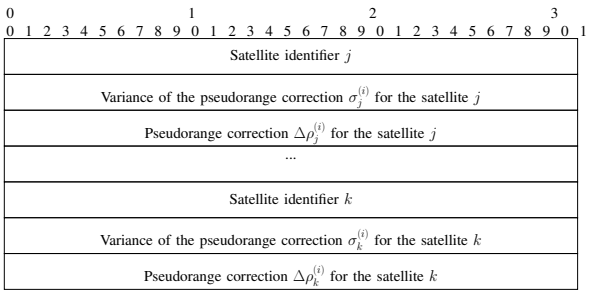

Fig. 3. Format of DDGPS application messages sent by branch nodes to their cluster leaf nodes and upstream branch node

downstream from node 5 which is downstream from node 6. Nodes 1, 2, and 4 are the leaf nodes belonging to the cluster of node 3 (*i.e.* node 3 is their branch node).

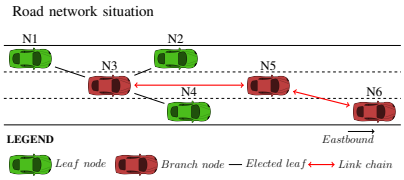

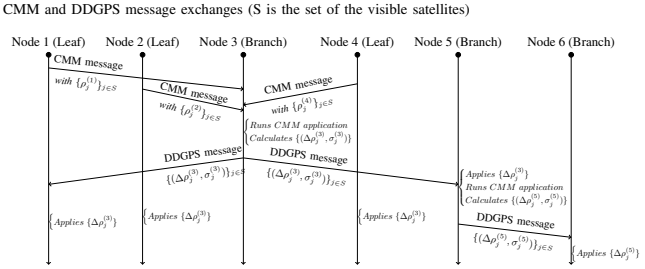

Fig. 4. Sequence of CMM-DDGPS application messages on a 6-node VANET

Firstly, leaf nodes 1, 2, and 4 send each one a CMM application message containing their pseudorange measurements with the satellite identifiers to their branch node (node 3). Then, after having processed CMM, then DDGPS algorithm, node 3 sends a DDGPS application message to both its cluster leaf nodes (nodes 1, 2, and 4) and the upstream branch node 5 with $\Delta\rho_j^{(3)}$ and $\sigma_j^{(3)}$ values. The receiver nodes recalculate and refine their position.

Next, as the branch node 5 has no leaves in its cluster, it just sends a DDGPS application message conveying an update of both the pseudorange correction and variance to its upstream branch node 6. The update takes into account the own pseudorange measurements of node 5.

As a conclusion, it is clear that this whole exchange sequence on CBL scheme contributes to the definition of the disjointed groups required by the DDGPS application.

V. Performance Evaluation

This section presents the performance evaluation of the proposed CBL scheme with CMM and DDGPS applications over varying network traffic conditions in a highway scenarios using OPNET Riverbed Modeler.

A. Road configuration

The road configuration used in this study consists of a 10-km section of the highway A27 that links Lille in France to Belgium (Fig. 5) and the by-way D90. The highway A27 is a two-lane two-way highway. The by-way D90 is a one-lane two-way road crossing perpendicularly the section of the highway. We got the real world traffic data recorded on the A27 on April 6th, 2017, by the French road infrastructure manager DIR Nord ("*Direction interdépartementale des routes du Nord*"). These data were measured by the electromagnetic loops placed inside the road A27. Fig. 6 shows the average number of vehicles per hour on the A27 section during the entire day while the Fig. 7 shows the data recorded per minute from 12:35 p.m.

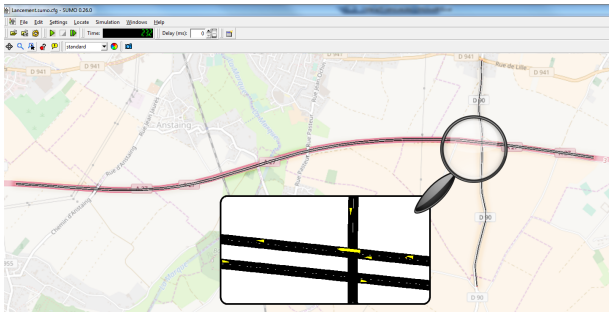

Fig. 5. SUMO modeling of the road network consisting of the two-lane two-way highway A27 (the horizontal road) and the one-lane two-way road D90 (the vertical road)

Two road networks were considered to evaluate the CBL behavior depending on whether the D90 road is taken into account or not in the simulation. The first road network assumes a vehicle density of 250 cars per hour on each traffic way of the road D90. The second road network assumes that the D90 is not taken into account. We designed three different traffic density cases for this evaluation. The first case corresponds to a variable traffic density observed in the A27 section from 12:35 p.m. (Fig. 7). The second case corresponds to a relatively low vehicle density. It takes fixed density values corresponding to the average value obtained on the section at 6:00 a.m. (Fig. 6). The third case corresponds to a relatively high vehicle density. It takes fixed density values corresponding to the average value obtained on the section at 7:00 a.m. (see Fig. 6). Four different scenarios with different traffic densities and road network cases are considered. The different scenarios, named R1, R2, R3, and R4, are listed in Table I.

The VANET node trajectories were generated with the SUMO software and the same parameters than those taken in our previous study [5].

B. Node configuration and network traffic models

The simulation platform of OPNET Riverbed Modeler has been used to evaluate the network performance. This section describes the node parameters and the network configuration.

The simulated system is an ad hoc network of vehicles equipped with IEEE 802.11p cards configured as described

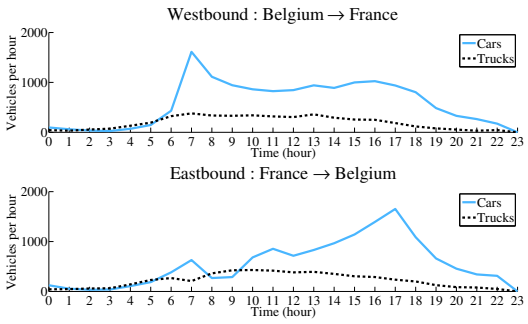

Fig. 6. Vehicle density averaged by the hour on the highway A27 on April 6th, 2017 obtained from electromagnetic loops placed in the road.

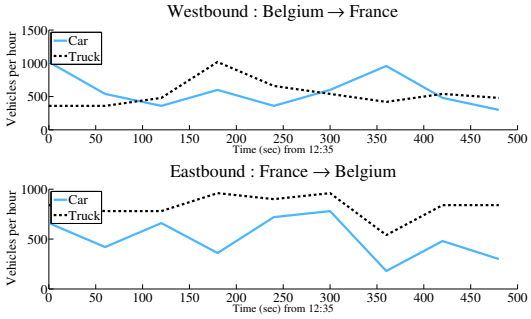

Fig. 7. Vehicle density on the highway A27 on April 6th, 2017 from 12:35 p.m., obtained from electromagnetic loops placed in the road.

TABLE I

SCENARIOS AND VALUES OF ROAD TRAFFIC DEMAND

Scenario	Road network	Vehicle density (veh/h)			
		Eastbound		Westbound	
		Car	Truck	Car	Truck
R1	A27 + D90	Variable density - Fig. 7			
R2	A27	Variable density - Fig. 7			
R3	A27	630	208	1620	380
R4	A27	380	260	430	320

in Table II. The transmission power is set at 0.005 W and the receiver sensitivity at -95 dBm in order to obtain a communication range of 500 m and to match the IEEE 802.11p dedicated short range communication. In order to take into account the velocity of VANET nodes, we used the half parameter value of those recommended by the RFC 3626 [6]. The Hello interval concerns the periodic Hello messages sent by every node to discover its one-hop neighbors. The Topology Control (TC) interval concerns the TC messages sent by every branch nodes. TC messages are used by each node in order to build and update its routing table. The implementations of 802.11p and OLSR used are those provided by the Riverbed OPNET Modeler. The CBL scheme has been implemented in a copy of the OLSR model code derived from [7].

C. OPNET performance metrics

Four performance metrics are considered:

TABLE II
NODE CONFIGURATION IN OPNET

Attribute	Value
Physical Characteristics	5.0 Ghz
Data Rate	13 Mb/s
Transmit power	0.005 W (i.e. 7 dBm)
Receiver sensitivity	-95 dBm
Transmission range	500 m
Hello interval	1 s
TC interval	2.5 s
Neighbor hold time (Vtime)	3 s (3*Hello interval)
Topology hold time	7.5 s (3*TC interval)
Duplicate message hold time	15 s

1) Nb_Branch, the total number of branch nodes in the network;
2) Nb_Leaf, the total number of leaf nodes in the network;
3) PDR, the packet delivery ratio which is the ratio of the number of successfully delivered packets to the number of the sending packets;
4) Delay, the "end-to-end delay" obtained during the simulation which concerns the time taken by a packet to reach its destination. It is measured as the difference between the arrival time of a packet at its destination and its creation time.

D. OPNET simulation results

We varied the scenario from R1 to R4 and the intervals for sending CMM and DDGPS messages from 50 ms to 500 ms with a sampling interval of 50 ms. We fixed the number of visible satellites at 12 satellites (in fact, the mean, minimal and maximal numbers of visible GPS satellites are respectively 10, 4 and 24 [8]). Thus, with a header of 128 bits defined in the OLSR protocol, the leaf nodes send a 896-bit CMM packet and the branch nodes a 1280-bit DDGPS packet. For each simulation configuration, made up of a scenario and a transmission interval, the simulation is run 10 times with different seed values for the OPNET random generator in order to avoid that the related sequence favors a particular situation.

Fig. 8 to 12 present the results for each performance metric. The simulations are run for 300 seconds, but the statistics are not recorded during the first 200 seconds, which is the time needed for the stabilization of the network [5]. Fig. 8 and 10 use a representation with box-plot where the central value of the box is the median, the rectangle edges are the quartiles and the vertical lines are calculated using 1.5 times the interquartile space.

Fig. 8 shows the numbers of leaf nodes and branch nodes in the network for each scenario. These numbers vary little in a same scenario. Indeed, the change of the sending periods of the CMM and DDGPS messages has no influence on the CBL protocol which elects the branch and leaf nodes. Scenario R1 counts about 50 branch nodes and 70 leaf nodes. Less nodes intervene in R2 since the traffic on road

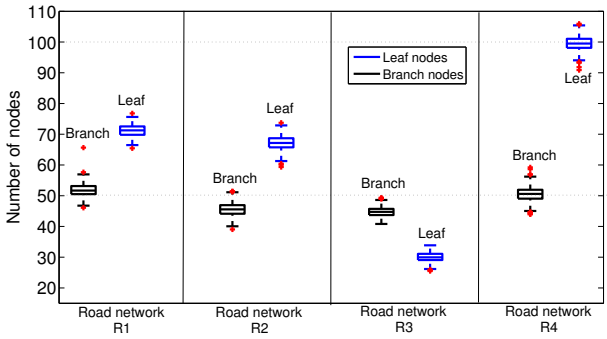

Fig. 8. Number of branch and leaf nodes in the network according to scenario R1, R2, R3, and R4.

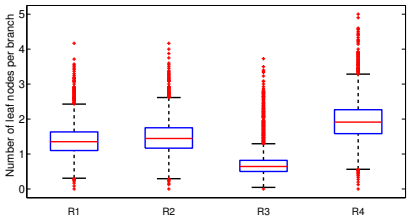

Fig. 9. Number of leaf nodes per branch in the network according to scenario R1, R2, R3, and R4.

D90 is not simulated (Table I). That explains the slightly lower numbers of leaf and branch nodes; R2 counts about 45 branch nodes. In R3, where the vehicle density is even lower than in R2, we observe that the number of leaf nodes decreases drastically from 65 to 30, while the number of branch nodes remains stable at about 45 nodes. Indeed, to create the chain structure, a sufficient number of branch nodes is necessary. Finally, R4 simulates the morning rush hour with a very high density of vehicles. The number of branch nodes increases slightly from R2 and R3, with a median of 45 nodes, to R4, with a median of 50. The number of leaf nodes explodes from 30 in R3 simulation to about 100 in R4. These results emphasize the behavior of the CBL routing protocol: as soon as the number of branch nodes is reached to create an unbroken chain for a specific road section, the other nodes remain leaf nodes. In this study, a dynamically stable chain is achieved with about 45 to 50 branch nodes. Each branch node receives CMM corrections from 1 to 5 leaf nodes (Fig. 9). Fig. 8 and 9 of the article [4] show that the GPS biais estimation error in distance ranges from 13.2 m for 1 neighbor node to 9.2 m for 5 neighbor nodes; and the standard deviation respectively varies from 5 m to 3.4 m. The improvement in the precision of the node positions and the level of confidence of this position increase with the number of the nodes in each cluster. Thus, the branch nodes with a higher number of leaf nodes provide the entire network with better corrections through DDGPS messages.

Fig. 10 shows the delay (a) and the packet delivery ratio (b) obtained in the simulation according to the scenario. We see that the delays are always below 250 ms, however many outsider points are out of the box-plot. The delays obtained for R1 and R2 are almost equivalent with a median

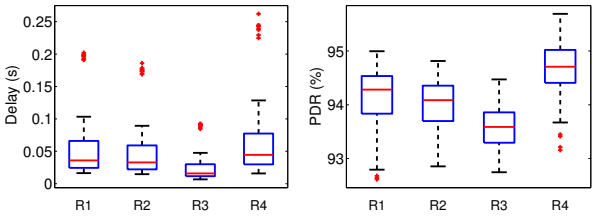

Fig. 10. (a): Delay obtained according to the scenario. (b): PDR obtained according to the scenario

value of 25 ms. The R3 scenario shows lower delays, while R4 displays the most important delays. Indeed, R4 has the highest density of nodes, which induces more packet collisions. The packet delivery ratio (PDR) ranges from 92.5% to 95.5% and is sensitive to the number of nodes: similar PDR results are obtained for R1 and R2 where the numbers of nodes are very close; it is the lowest for R3; and the highest for R4 which has the highest number of nodes.

Fig. 11 and 12 provide the evolution of delays and PDR according to the sending interval, respectively. In Fig. 11, the profile of the curves is very similar regardless of the scenario: delays decrease when the sending interval increases. Indeed, the smallest the value of the sending interval, the more important the number of the transmitted application messages, which overloads the communication network, leading to longer delays. Let's note that the delay values obtained for the sending period of 50 ms corresponds to the outsider points identified in Fig. 10(a). Maximum aberrant delay points are noted. These aberrant values are due to singular situations, and are not representative compared to the numerous values close to the respective averages.

Fig. 12 provides the evolution of the PDR according to the sending interval. The profile of the curves is very similar regardless of the scenario: PDR increases with the sending interval value. Indeed, the smaller the value of the sending interval, the higher are the number of application messages which overloads network, and leads to a lower PDR.

VI. Conclusion

Previously, we proposed a clustering scheme for vehicular ad hoc networks that outperformed the multipoint relaying technique (MPR) in OLSR in terms of routing traffic flooding optimization, and end-to-end delay. In this work, we have presented a distributed location application that improves GPS location information, provided that disjoint groups of vehicles cooperate and exchange their location information and the related correction in order to improve their own location. We have shown that, besides providing an accurate organization through the groups formed by each branch node and its leaf nodes, CBL provides an accurate V2V communication service to the vehicles. The results of the performance evaluation, achieved with real-world road traffic scenarios of various densities, show that the end-to-end delays provided to the distributed application are acceptable even for the highest traffic rate, and that the PDR remains higher than 92%. These results are obtained in presence

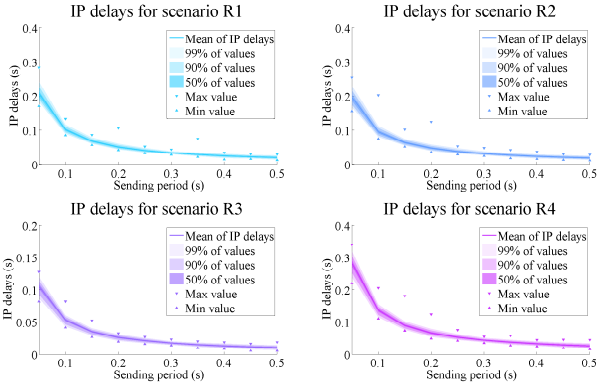

Fig. 11. Delay obtained according to the scenario and the sending period

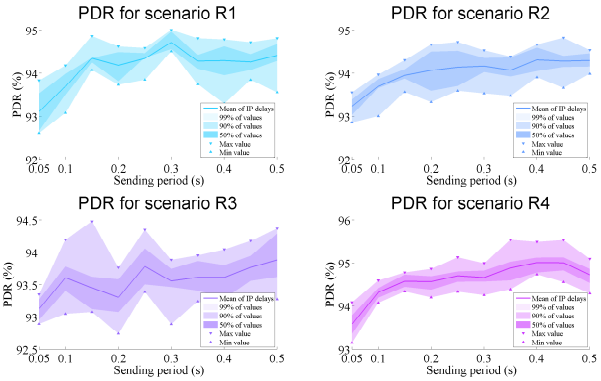

Fig. 12. PDR obtained according to the scenario and the sending period

of OLSR routing traffic including CBL-specific information. In future work, we will investigate the performance of this location application in presence of other concurrent safety or driving-assistance application traffic.

References

[1] E. Kaplan and C. Hegarty, *Understanding GPS: principles and applications*. Artech house, 2005.

[2] A. Boukerche, H. A. Oliveira, E. F. Nakamura, and A. A. Loureiro, "Vehicular Ad Hoc Networks: A New Challenge for Localization-Based Systems," *Computer Communications*, vol. 31, pp. 2838–2849, July 2008.

[3] E. Pollard and D. Gingras, "Improved Low Cost GPS Localization By Using Communicative Vehicles," in *2th International Conference on Control, Automation, Robotics and Vision, ICARCV*, (Guangzhou, China), Dec. 2012.

[4] M. Rohani, D. Gingras, and D. Gruyer, "A Novel Approach for Improved Vehicular Positioning Using Cooperative Map Matching and Dynamic Base Station DGPS Concept," *IEEE Transactions on Intelligent Transportation Systems*, vol. 17, no. 1, p. 10, 2016.

[5] L. Rivoirard, M. Wahl, P. Sondi, M. Berbineau, and D. Gruyer, "Chain-Branch-Leaf: A clustering scheme for vehicular networks using only V2V communications," *Ad Hoc Networks*, vol. 68, pp. 70–84, Jan. 2018.

[6] T. Clausen, P. Jacquet, C. Adjih, A. Laouiti, P. Minet, P. Muhlethaler, A. Qayyum, and L. Viennot, "Optimized link state routing protocol (OLSR)," *IETF*, no. RFC 3626, 2003.

[7] P. Sondi, D. Gantsou, and S. Lecomte, "A multiple-metric qos-aware implementation of the optimised link state routing protocol," *IJCNDS*, vol. 12, no. 4, pp. 381–400, 2014.

[8] A. Martineau, C. Macabiau, and M. Mabilleau, "GNSS RAIM assumptions for vertically guided approaches," in *GNSS 2009, 22nd International Technical Meeting of The Satellite Division of the Institute of Navigation*, (Savannah, United States), pp. 2791–2803, Sept. 2009.